STM JOURNALS

Journal of
Polymer & Composites

ISSN: 2321-2810 (Online)
ISSN: 2321-8525 (Print)
Volume 14, Issue 2, 2026
DOI (Journal): 10.37591/JoPC

https://journals.stmjournals.com/jopc

Research JoPC

Advanced Liquid Crystal Polymer Substrate for Flexible Antenna Design

Jitender Kumar[1], Priyanka Gupta[2,*], Jatin Gaur[3], Neera Aggarwal[4], Yogita Arora[5], Sourabh Rana[6]

Abstract

A type of thermoplastic polymers known as liquid crystal polymers (LCPs) is frequently used to package millimeter (mm)-wave, microwave, and radio frequency (RF) integrated circuits that operate at frequencies as high as 60GHz. LCPs are of prospective relevance as packaging material for advanced circuits at mm-wave frequencies due to their appealing electrical, thermal, and mechanical qualities and comparatively low cost. Flexible and conformal antennas are made possible by LCP's exceptional mechanical flexibility and endurance. Applications in wearable technology, flexible electronics, and small communication systems can benefit from this feature. The literature review indicates that existing flexible antennas for millimeter-wave applications either have limited impedance bandwidth or poor impedance matching, and no design has been reported that successfully accomplishes both at the same time. This work presents a flexible antenna design for millimeter-wave applications utilizing a single-port coplanar waveguide (CPW) feed mechanism on an LCP substrate. The proposed antenna has a dimension of 22.5×22.5×0.1 $\boldsymbol{mm^3}$*, operating band of 4.879-5.513GHz, 8.394-10.006GHz, and 13.864-39.892GHz. The simulated results show that the impedance bandwidth (S11 < −10dB) covers three frequency bands whose fractional bandwidth of 12.21%, 17.51%, and 96.8% and the antenna exhibits an average 5dBi peak gain and stable broadside radiation at 5.2, 9.2, and 26.9 GHz, indicating dependable multiband directional performance with low distortion. Moreover, antenna is simulated at bending radii of 10 mm, 30 mm, and 50 mm in order to assess its flexibility. Reliable performance under bending conditions is confirmed by the results, which show a slight shift in resonant frequency and steady impedance matching.*

Keywords: Millimeter (mm)-wave, liquid crystal polymer (LCP), radio frequency, coplanar waveguide, polymers

INTRODUCTION

"Wireless communication systems have rapidly advanced in recent years, and planar printed antennas have garnered significant attention in both academic and industrial fields due to their compact size, lightweight nature, ease of fabrication, and straightforward integration [1]. Polymer composites are a significant class of sophisticated materials formed by integrating a polymer matrix with reinforcing components. This amalgamation yields enhanced mechanical, thermal, electrical, and additional functional attributes. These materials have considerable benefits compared to conventional monolithic materials, like metals and ceramics, owing to their enhanced strength-to-weight ratio, durability, and customized performance [2, 3]. Although millimeter-wave (mm-wave) MIMO and beamforming antenna

***Author for Correspondence**
Priyanka Gupta
E-mail id: priyankagupta09@gmail.com

[1-3,6]Assistant Professor, Department of Electronics and Communication Engineering, Bharati Vidyapeeth's College of Engineering, New Delhi, India
[4,5]Associate Professor, Department of Electronics and Communication Engineering, Bharati Vidyapeeth's College of Engineering, New Delhi, India

Received Date: March 17, 2026
Accepted Date: March 26, 2026
Published Date: April 29, 2026

Citation: Jitender Kumar, Priyanka Gupta, Jatin Gaur, Neera Aggarwal, Yogita Arora, Sourabh Rana. Advanced Liquid Crystal Polymer Substrate for Flexible Antenna Design. Journal of Polymer & Composites. 2026; 14(2): 233–245p.

systems have made significant strides, current designs primarily rely on stiff substrates like PTFE and RO4350B, creating large multilayer structures that are difficult to integrate into small and portable devices. Moreover, large insertion losses at mm-wave frequencies cause commonly used materials like FR-4 and Rogers laminates to have lower radiation efficiency. Additionally, their high moisture sensitivity and restricted flexibility limit their use in environmentally stable and conformal systems. While several methods have been put forth to improve MIMO performance, they frequently depend on larger element spacing or intricate decoupling mechanisms, which compromises design simplicity and compactness [4]. Liquid Crystal Polymer (LCP), on the other hand, provides great moisture resistance, reduced dielectric loss, and outstanding flexibility [5].

Polymer Materials for RF Devices

Because polymer materials provide low dielectric loss, lightweight structure, flexibility, and strong thermal stability, they are frequently employed in radio frequency (RF) and microwave devices. In integrated circuits, transmission lines, and antennas, these materials serve as substrates or insulating layers. Liquid crystal polymer (LCP), polyimide (PI), polytetrafluoroethylene (PTFE), and epoxy-based laminates are common polymers utilized in radiofrequency devices. They are appropriate for high-frequency applications such satellite communication systems, radar, 5G, and 6G due to their stable dielectric characteristics [27]. The foundation material used to create electrical circuits and components is called a polymer substrate. Polymer substrates give conductive layers in electronics both mechanical support and electrical insulation. Polymer substrates are more flexible, lighter, and simpler to produce than conventional materials like glass or ceramic. Glass fibers, carbon fibers, or ceramic particles are examples of reinforcing elements that are combined with a polymer matrix to create polymer composites. These reinforcements improve the polymer's dielectric qualities, mechanical strength, and thermal stability [6, 7].

FR4 substrates, while widely adopted in antenna design due to their cost-effectiveness and ease of manufacturing, present significant disadvantages when employed in millimeter-wave (mm-wave) band applications. These drawbacks primarily stem from their intrinsic material properties at higher frequencies, leading to compromised antenna performance in terms of efficiency, signal integrity, and stability. The foremost disadvantages of FR4 substrates in the mm-wave band is their high dielectric loss. Dielectric loss refers to the energy dissipated as heat within the substrate material when exposed to an alternating electric field, which becomes more pronounced at higher frequencies. This high loss tangent in FR4 materials leads to significant signal attenuation, thereby reducing the overall radiation efficiency of antennas designed on them. For instance, comparative analyses have shown that antennas fabricated on FR4 substrates exhibit lower radiation efficiency [2–5].

Features of Liquid Crystal Polymer

Because of their distinct molecular structure, liquid crystal polymers are well known for their remarkable mix of mechanical, thermal, and electrical capabilities. The scientific literature often reports that LCPs have one of the lowest dielectric constants among high-performance thermoplastics. The relative permittivity (ε_r) of aromatic polyester-based LCPs usually varies from 2.9 to 3.2 for frequencies between 1 MHz and 10 GHz, according to experimental research employing resonant cavity methods and impedance spectroscopy. The highly organized, anisotropic molecule structure that reduces polarizability and dipole mobility in the direction perpendicular to the chain axis is responsible for this low number. Because of their low dielectric loss tangent ($\tan \delta$), which is frequently less than 0.004 at microwave frequencies, LCPs are perfect for high-frequency applications where signal integrity is crucial. Another characteristic of LCPs is their thermal stability; under nitrogen atmospheres, breakdown temperatures consistently exceed 400°C in thermogravimetric analysis (TGA) experiments. Moisture resistance in LCPs is exceptional due to their highly hydrophobic nature and dense molecular packing. Gravimetric water absorption tests following ASTM D570 standards consistently report equilibrium moisture uptake values below 0.04% after 24 hours of immersion in water at 23°C [6].

Liquid Crystal Polymer (LCP) substrates present notable advantages for millimeter-wave (mm-wave) antenna design due to their favorable electrical and mechanical properties, addressing critical challenges in high-frequency communication systems. The design of mm-wave antennas for applications such as 5G and beyond necessitates materials with low dielectric constant, low loss tangent, excellent thermal stability, and flexibility [6].

Significance of Polymer in Antenna Performance

The mechanical features of polymers allow for whole new antenna paradigms in addition to their dielectric qualities. The development of conformal antennas that can be incorporated into wearable electronics, implantable medical devices, and aerospace structures with intricate curvatures is made easier by flexible and stretchable polymers such as thermoplastic polyurethanes (TPUs), polyethylene terephthalate (PET), and polydimethylsiloxane (PDMS). These flexible substrates allow antennas to bend, twist, or stretch without significantly degrading their radiation properties because they maintain consistent electrical performance even under mechanical deformation [7, 8]. Innovative fabrication methods like roll-to-roll processing and inkjet printing, which lower manufacturing costs and enable large-scale production of antenna arrays, are also made possible by the mechanical flexibility. LCP meets these requirements, facilitating efficient signal transmission, compact designs, and integration with flexible electronics. Its moisture resistance and mechanical robustness further enhance the reliability of mm-wave antennas in diverse environmental conditions [9]. Millimeter(mm)-wave frequencies, typically ranging from 20 GHz to 300 GHz, are increasingly crucial for next-generation wireless communication due to their capacity for high data rates and large bandwidths. In biomedical applications, the adjustment of polymer composition, thickness, and microstructure directly affects important antenna parameters like as bandwidth, polarization purity, impedance matching, and specific absorption rate (SAR). Although thinner polymer substrates typically lower dielectric losses, they may jeopardize mechanical integrity, necessitating careful trade-off analysis during the design process. [10, 11]. However, these frequencies are susceptible to significant signal loss and require highly efficient antennas with specific characteristics [9], [12]. The performance of antennas in this spectrum is heavily influenced by the substrate material [6]. The antenna has a diminutive inner rectangular ring, an outer rectangular loop including three slits, and a parasitic strip [13]. Four concentric pentagon-shaped slots that are equally spaced are used to make up the antenna design and excites via a power divider structure for millimeter(mm)-wave frequency band [14]. Many current designs seek to achieve both improved isolation between closely spaced antenna elements and multi-band performance. On [15, 16]. There was reported another design of a millimeter-wave 5G antenna that used a dual-feed square loop design, operated at 38 GHz and 75 GHz, had a gain of about 3 dBi, and had a fractional bandwidth of 14% [17]. Further many antennas reported that rely on CSRRs, DGS, EBGs, parasitic or slot elements, or decoupling networks [18–20]. Later research offers a decoupling method to improve isolation in a millimeter-wave DRA-based antenna [21, 22].

DISCUSSION ON POLYMER CHARACTERIZATION

Dielectric materials are essential to the operation and performance of many radio frequency (RF) and microwave devices, especially antennas and resonators, which are essential for contemporary wireless communication systems like 5G and sensing applications. Key device factors including bandwidth, efficiency, and resonance frequency are directly determined by the properties of these materials, such as physical thickness, loss tangent (tanδ), and relative permittivity ($\in_r$). The design, optimization, and shrinking of high-performance RF components depend on an understanding of these interactions [23, 24].

In Table 1, reduced dielectric constant increases fringing fields, resulting in an expanded bandwidth, yet a low loss tangent enhances radiation efficiency. Substrate thickness affects effective permittivity and induces resonance shift, as elaborated in [24]. Establishing the structure-property links that control material performance across scientific and engineering fields require a thorough discussion section on polymer characterization [25–27]. This analytical approach provides a multifaceted view of polymeric materials by integrating complementary methodologies to investigate chemical composition, molecular

architecture, thermal behavior, crystalline morphology, and surface topography. Spectroscopic techniques, especially Fourier-transform infrared (FTIR) spectroscopy, which detects functional groups and tracks chemical processes using distinctive vibrational modes, are the foundation of chemical characterization [28]. In this work, main goal is to suggest a compact antenna design that can handle the multiband operation required by contemporary communication systems while being smaller than those documented in earlier research. Each of the two modified elements in the suggested design is implemented as a compact etched patch. A range of 5G-based wireless communication applications are supported by this compact antenna. Liquid crystal polymer (LCP) has been utilized as a substrate in the suggested antenna design. Flexible LCP dielectric material, that has advantages of low, consistent dielectric constant across an extensive frequency spectrum, minimal thermal expansion coefficient, and reduced manufacturing costs. It is easy to fabricate into RF-integrating devices, which is suitable for printed antennas. An antenna based on LCP substrate material was reported without flexibility analysis [23]. Another large-sized LCP substrate-based antenna was reported [24]. This research presents a new compact LCP based tri-band antenna for use in Beyond-5G (B5G) communication, Advanced 5G/6G communication, 5G mm-wave communication (FR2 extension bands), and 6G communication bands (planned for future networks). The antenna is printed on a 0.1 mm LCP substrate and has an overall size of 22.5 × 22.5 × 0.1 mm. This makes it smaller than a standard rigid antenna and capable of operating in a bending condition. Additionally, improving antenna integration are made possible by positioning the radiation patch on the top surface of the LCP substrate.

LCP BASED FLEXIBLE ANTENNA DESIGN AND ANALYSIS

By adding additional horizontal rectangular shaped slot to the main radiation patch, an effective tri-band for Beyond-5G (B5G) communication, 5G mm-wave communication (FR2 extension bands), Advanced 5G/6G communication, and 6G communication bands (proposed for future networks). The antenna design, parameter analysis, and simulated outcomes, such as S11, S12, and radiation patterns, are all covered in detail. Furthermore, the suggested antenna is simulated, and the results are examined under various bending conditions. For mm-Wave antenna performance, material selection is crucial. This includes low-loss substrates like liquid crystal polymer (LCP). Key issues for mm-Wave antenna systems include propagation path constraints, power consumption and thermal control in highly integrated systems, cost–performance trade-offs for mass production, and interoperability standardization between vendors.

In Table 2, the center frequencies of the proposed tri-band antenna are 5.19 GHz, 9.20 GHz, and 26.88 GHz, respectively, covering WLAN, X-band, and wide mm-wave applications. Wide millimeter-wave and ultra-wideband (UWB) frequency bands are partially used by the planned antenna. No previously documented antenna supports both UWB and mm-wave frequency activities, according to the literature review.

Table 1. Antenna parameters and performance relations.

Parameters	Value leads to	Effects
ϵ_r	Lower ϵ_r	Wide Bandwidth
Loss tangent ($tan\delta$)	Lower $tan\delta$	Higher Efficiency
Thickness (h_s)	Thin Substrate	Frequency Shift

Table 2. Operating frequency band the proposed multi-band antenna.

Band	Frequency Range (GHz)	Center Frequency (GHz)	Bandwidth (GHz)	Fractional BW (%)	Major Applications
Band-1	4.879 – 5.513	5.2	0.6348	12.21	5-GHz WLAN, Wi-Fi (IEEE 802.11a/ac/ax)
Band-2	8.394 – 10.006	9.2	1.6111	17.51	X-band radar, satellite communication
Band-3	13.864 – 39.892	26.9	26.028	96.8	5G mm-Wave, Ku/K/Ka-band satellite, high-speed links

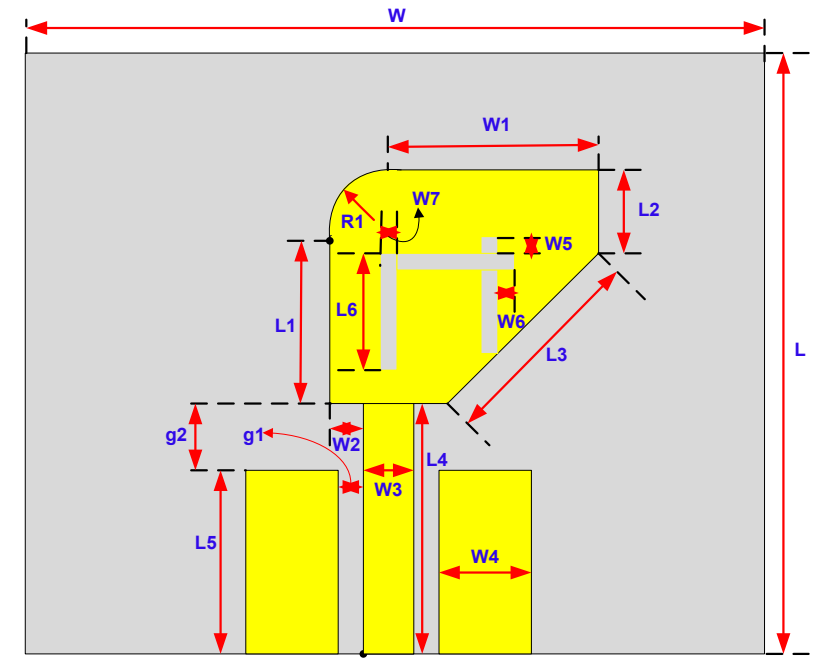

Top View

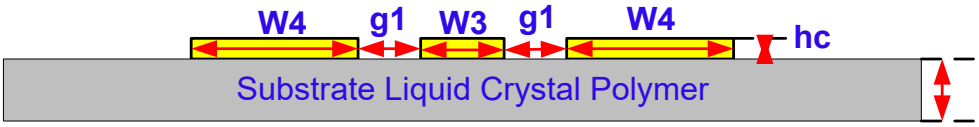

Front View

Figure 1. Schematic diagram of proposed antenna.

This study presents a tri-band antenna based on LCP supplied by a compact coplanar waveguide (CPW) for WLAN, X-band, and 5G mm-wave applications. The antenna is simulated on a 0.1 mm thick LCP substrate and has an overall size of 22.5 × 22.5 × 0.1 mm. This makes it smaller than the conventional rigid antenna and capable of operating in the bending condition. For improved impedance matching and a wider working bandwidth, it is fed via a CPW. Additionally, to enhance antenna integration and lower production costs, the ground plane and radiation patch are designed on the same side of the LCP substrate. An effective triple band for WLAN, X-band, and 5G systems is created by adding an extra F-shaped slot, bending and chamfering the edges to the primary radiating patch and the coplanar waveguide ground. Additionally, Computer Simulation Technology (CST) software simulates the antenna performance on various bending radii.

LCP ANTENNA PARAMETERS

Figure 1 depicts the design antenna's geometry. The suggested antenna is built on an LCP substrate with a relative permittivity of 3.1 and supplied with CPW with a thickness of 0.1 mm. The antenna is 22.5 × 22.5 mm^2. The F-shaped slot in the upgraded patch antenna is resonating at three different frequencies. The broad mm-wave frequency range is caused by an F-shaped slot. Simulation studies are done and all optimized parameters of designed antenna are shown in Table 3.

Figure 2 illustrates how the various Stages change to describe the design process of the suggested antenna. The CPW feed line is positioned alongside a modified patch antenna construction. The inverted F-shaped slots in the redesigned patch structure are excited for various frequency bands.

Table 3. Geometric parameters of proposed antenna.

Parameter	Value (mm)	Parameter	Value (mm)
L	22.5	W	22.5
L1	7	L2	3.3
L3	6.53	L4	8.75
L5	8	L6	3.5
W1	7	W5	0.73
W3	0.5	W2	1
g1	0.2	W4	2
R1	0.5	g2	0.75
hc	0.035	hs	0.1

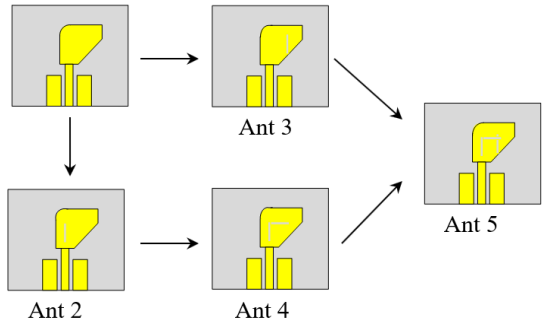

Figure 2. Implement procedure for design antenna.

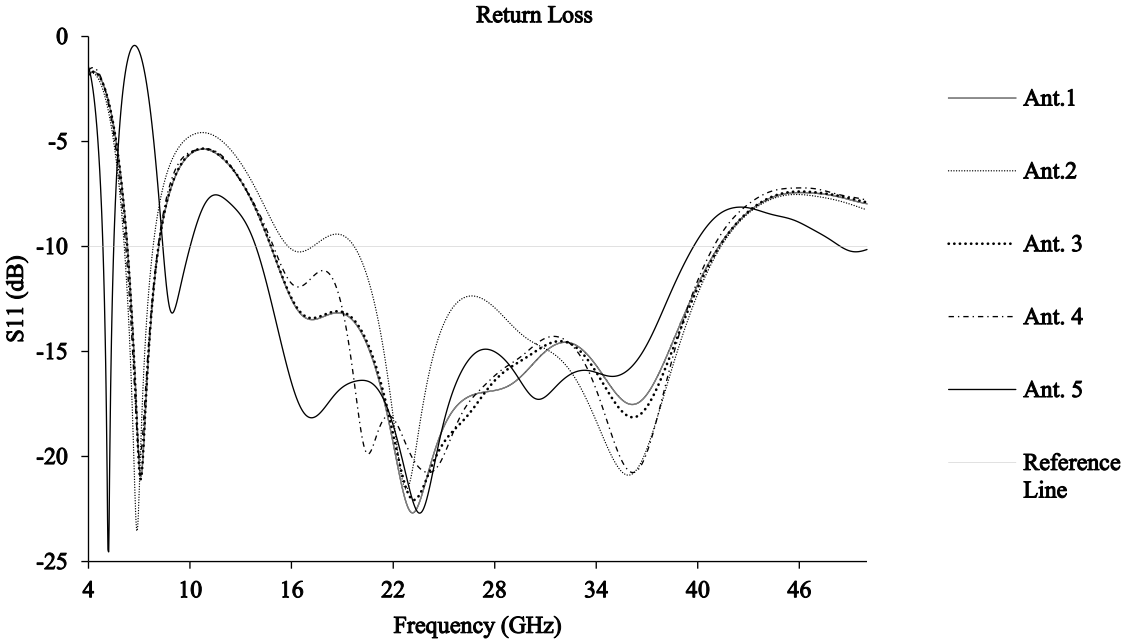

Figure 3. S_{11} shows the different antennas included in the simulation.

The design process is shown in Figure 2. Figure 3 displays each antenna's S11 curve. The fundamental rectangular antenna equations [25, 26] determine the rectangular patch's length and width. Each strip's (L6) length of inverted-F can be computed as follows and is found to be almost a quarter of the dielectric wavelength determined at the appropriate resonant frequency:

$$L = \frac{C}{2f_r\sqrt{\varepsilon_{eff}}} - 2\Delta L \quad (1)$$

$$\varepsilon_{eff} = \frac{(\varepsilon_r+1)}{2} + \frac{(\varepsilon_r-1)}{2}\left(1 + \frac{12h}{W}\right)^{-0.5} \quad (2)$$

$$\Delta L = 0.412h\frac{(\varepsilon_{reff}+0.3)(\frac{W}{h}+0.264)}{(\varepsilon_{reff}-0.258)(\frac{W}{h}+0.8)} \quad (3)$$

$$L = \frac{C}{2f_r\sqrt{\varepsilon_{reff}}} - 2\Delta L \quad (4)$$

Where C is the speed of light, f_r is the desired resonant frequency, and $\varepsilon_{eff}$is the effective relative permittivity. The antenna design starts with a simple rectangular monopole antenna (see Ant1) with a CPW-fed that can reach a frequency bandwidth from 4.879–5.5138GHz, supporting 5G and the 5.1964GHz WLAN standard. Because of the increased capacitance, Ant. 2 with a single half-wavelength slot is employed to achieve resonance at a lower frequency band. Ant. 3 is tuned to achieve resonance at the millimeter-wave band with a single slot at a different location. Ant. 4 uses an inverted L-shaped slot design to achieve a large bandwidth at a high frequency. Combine ant. 3 and ant. 4 to obtain the third resonance in the x-band in ant. 5.

The third resonance at the 9.2GHz X-band was obtained by simulating S11 of Ant. 5. Additionally, Antenna 5 maintained the wide frequency range produced by the original rectangular monopole antenna while operating at three distinct frequencies: 5.2GHz, 9.2GHz, and 26.9GHz. To make the modified rectangular structure resonate almost on the fundamental mode, the length of the slots on the radiating patch varies. The antenna's electric field distribution can be used to study its resonant properties. The antenna's simulated field distribution at frequencies of 5.2, 9.2, and 26.9 GHz is displayed in Figure 5. The current is primarily spread in the right slot, as seen in Figure 4(a). In Figure 4(b), the left slot contains the majority of the field.

The outcome demonstrates that the formation of two resonance modes in the lower band and middle band, respectively, is most significantly influenced by the right and left slots. As shown in Figure 4(c), the field distributed at the inverted F-slots of the modified rectangular patch, especially on three slots, which means that those parts affect the upper frequency band.

The field of the CPW transmission line at various frequency points is substantial in Figure 5, signifying that the antenna is operational and exhibits favorable impedance matching. Figure 5 displays the impedance characteristics of the aforementioned antenna, and it is evident that the operating band has good impedance matching. Based on the present distribution of the aforementioned three frequencies, the simulation of input impedance (real and imaginary) analysis is illustrated in Figure 5. The impedance characteristics of the aforementioned antenna are illustrated in Figure 5, demonstrating effective impedance matching within the operational band.

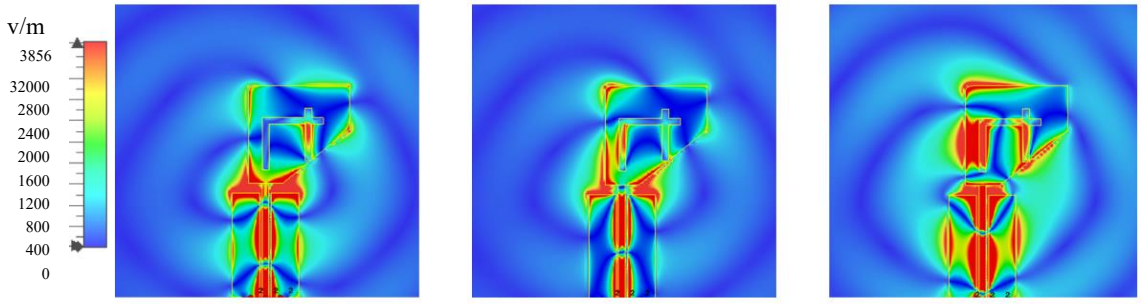

(a) 5.2GHz (b). 2GHz (c) 26.9GHz

Figure 4. Simulated field distribution of the proposed antenna at (a) 5.2, (b) 9.2, and (c) 26.9GHz.

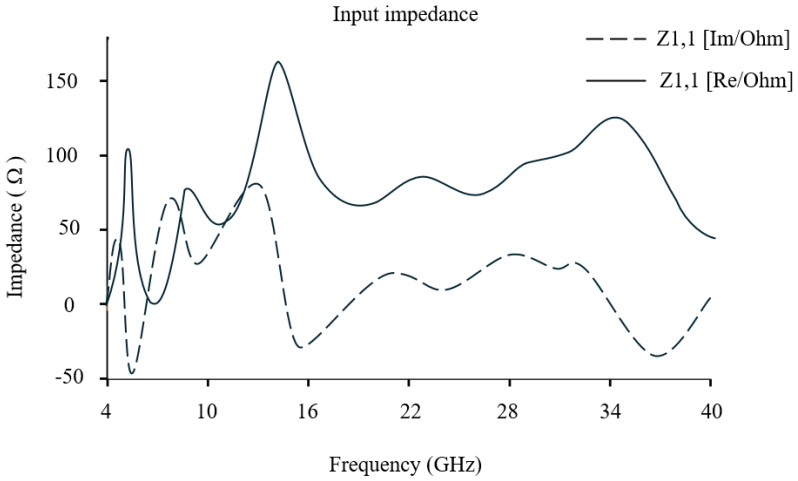

Figure 5. Input impedance curves of the proposed antenna.

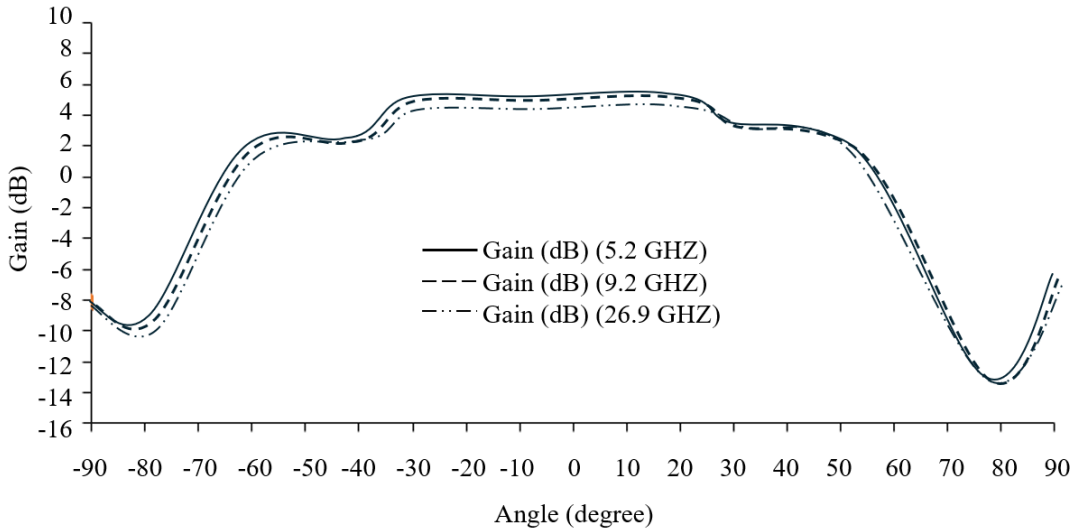

Figure 6. Simulated H-plane radiation pattern.

The proposed antenna's radiation properties were assessed at three different operating frequencies: 5.2 GHz, 9.2 GHz, and 26.9 GHz. Figure 6 shows the corresponding gain patterns. The findings show that all three frequencies have a radiation distribution that is primarily broadside, with maximal gain happening close to 0°. With peak gain values of roughly 5 dB at 5.2 GHz, 4 dB at 9.2 GHz, and 6 dB at 26.9 GHz, forward-directed radiation performance is constant throughout the multiband spectrum.

The antenna's structural symmetry and excellent impedance matching are confirmed by the patterns, which are essentially constant across frequencies. Beyond ±60°, the gain gradually decreases before sharply declining around ±80°. This is typical of planar radiators, where larger off-axis angles result in increasing edge diffraction and surface-wave effects. All things considered, the multi-band gain response verifies that the antenna attains dependable directional performance with low distortion in all desired frequency bands

The higher-frequency band is significantly impacted by the liquid crystal polymer's thickness. Figure 7 demonstrates that as the polymer substrate thickness (h_s) varies, the two resonances appear at higher frequency band, while the other two resonances in the lower-frequency band stay the same.

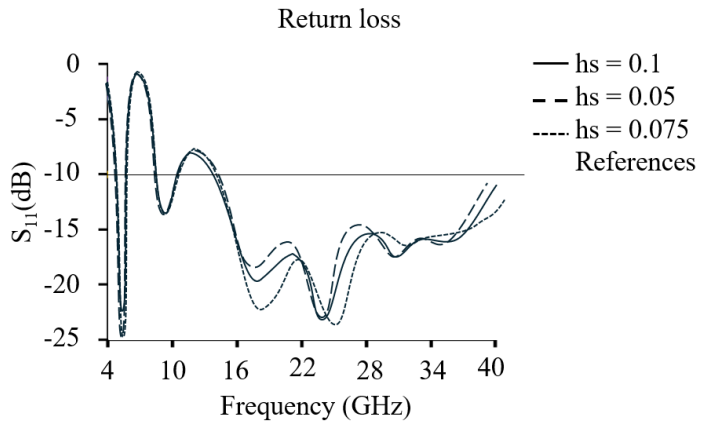

Figure 7. Simulated $S_{11}$with different values of polymer substrate thickness (h_s).

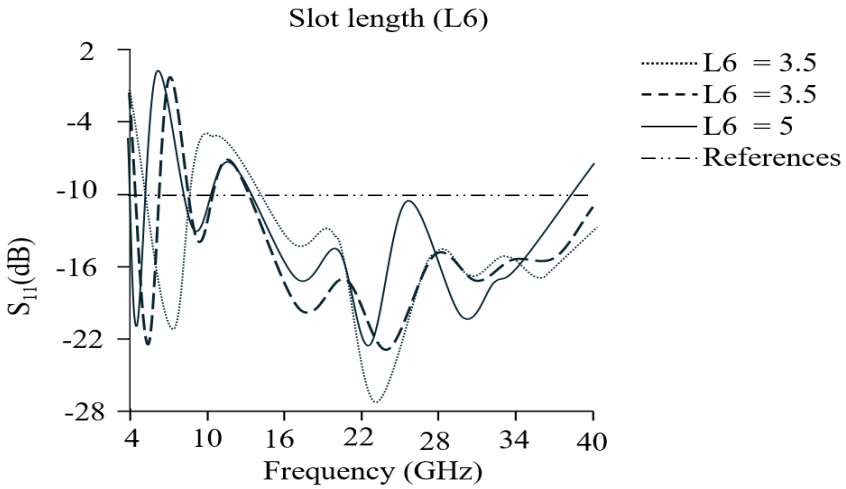

Figure 8. Simulated $S_{11}$with different values of radiating patch slot length (L_6).

Figure 8 illustrates that the augmentation of L_6 not only facilitates effective impedance matching in the lower frequency region but also alters the resonance of the proposed antenna. The augmentation of L_6 results in an increase in capacitance, hence shifting the band to lower frequencies. Consequently, by modifying the length of L_6, the middle and lower bands can be altered. The alteration in length solely impacts the associated frequency band, leaving other bands unaffected.

LCP BASED FLEXIBLE ANTENNA PERFORMANCES

The electromagnetic boundary conditions around the structure are altered when the antenna is bent over a curved surface, which has a direct impact on radiation behavior, resonance, and impedance matching. The return-loss performance of the antenna bent across a cylindrical surface with a curvature radius of R=10mm is shown in the Figure 9. Effective impedance matching under the bending situation is confirmed by the S_{11} curve, which shows three different resonant frequencies, all of which lie far below the −10 dB reference line. Strong energy coupling and little reflection are shown by the resonances, which occur around 7 GHz, 14 GHz, and 26 GHz, with the deepest null approaching −45 dB.

The antenna's flexibility and structural adaptation are highlighted by the accompanying 3D model, which shows the antenna construction conformally installed on the curved substrate of radius 10mm. Overall, the findings confirm that even under mechanical deformation, the antenna retains consistent multiband performance and appropriate return-loss behavior. Resonant frequency, return-loss depth,

and current distribution all somewhat alter as a result of bending. Nonetheless, the antenna maintains robust multiband performance with S_{11}well below the –10 dB threshold for R=10mm, demonstrating that the design can withstand curvature without experiencing appreciable degradation.

Figure 9 illustrates the S_{11} behavior under various bending circumstances. When R increases, the simulated S_{11} of the antenna impedance matching improve at middle and lower frequency bands. When R=10mm the simulation results show that the antenna can maintain the tri-band operation and shows improvements in impedance matching of middle and upper frequency band. But at lower frequency band impedance matching deteriorated due to bending of antenna. Meanwhile, the antenna maintains its tri-band operation and resonance frequency while it undergoes bending analysis. When R=30mm the simulation results show that the antenna can maintain the tri-band operation and shows improvements in impedance matching at lower, middle and upper frequency band and found none shift in resonance frequency at this bending condition also.

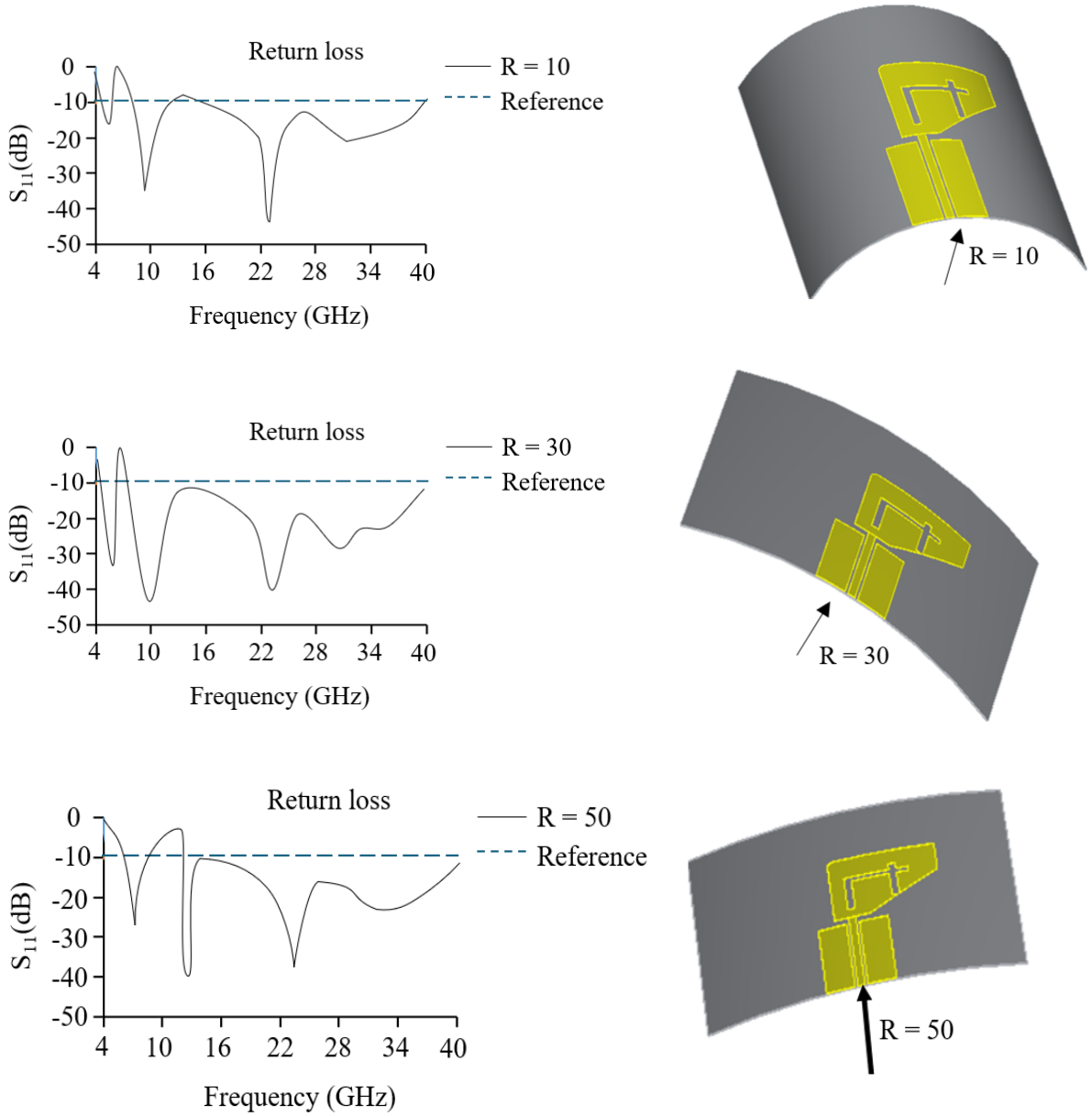

Figure 9. Simulated E-plane S_{11} for the proposed antenna rolled on a cylinder with three different radii configuration.

When R=50mm the simulation results show that the antenna can maintain the tri-band operation and shows improvements in impedance matching at lower, middle and upper frequency band, found shift in resonance frequency at lower and middle frequency band, and bandwidth of lower and upper frequency band increase at this bending condition.

In Figure 10, all examined bending radii reveal that the antenna exhibits significant robustness, as indicated by the close resemblance of the gain patterns, demonstrating great structural integrity and electromagnetic stability under mechanical deformation. The maximum gain continuously falls within the 4–6 dB range for core angular regions between –20° and +30°, indicating that the primary radiation characteristics are generally maintained despite the antenna's curvature. At the extremes (±90°), the gain diminishes to roughly –11 dB, indicative of diminished radiation efficiency in lateral directions for tiny flexible antennas. Moreover, when the bending radius increases-resulting in less curvature, the gain response becomes more uniform, and the discrepancies among the curves significantly lessen, with the profiles for R = 30 mm and R = 50 mm displaying negligible variation. Significantly, even under the most extreme bending condition of R = 10 mm, the antenna preserves an acceptable forward gain and maintains a steady angular radiation profile, highlighting its appropriateness for flexible and conformal wireless applications.

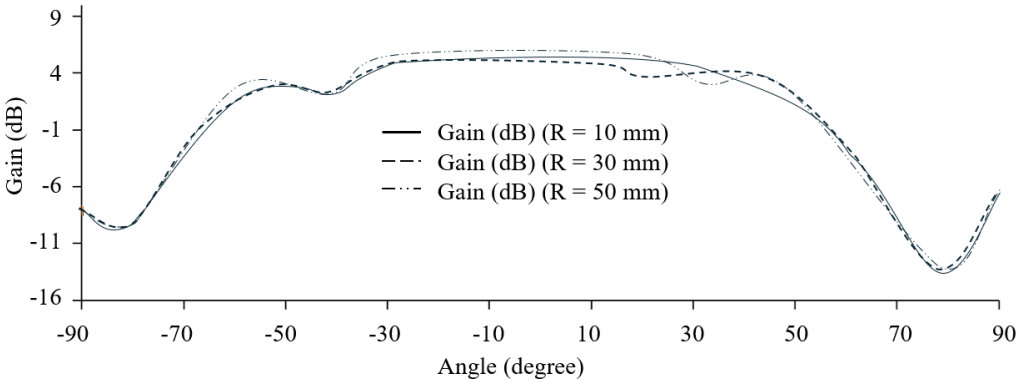

Figure 10. Gain versus angle comparison for the antenna under three bending radii (R = 10 mm, 30 mm, and 50 mm).

Table 4. Comparison of proposed antenna characteristics with existing design**.**

Ref.	Dimensions (mm^2/mm^3)	Return Loss (S_{11})	Substrate	Flexibility	Frequency Band	Design Simplicity
[2]	40 × 40 × 1.6 mm³	−18.2 dB @ 3.5 GHz	FR4 / RT-Duroid	Rigid	Sub-6 GHz	Moderate
[3]	45 × 35 × 1.6 mm³	−16.5 dB @ 2.45 GHz	FR4 / RT-Duroid	Rigid	Sub-6 GHz band	Simple
[5]	28 × 28 mm²	−20.4 dB @ 28	SIW–DRA substrate	Rigid	mm-Wave (28/38 GHz)	Complex
[8]	28 × 28 mm²	−26.1 dB @ 28 GHz	Rogers-type substrate	Rigid	mm-Wave (5G)	Complex
[9]	60 × 20 mm²	−21.4 dB @ 38 GHz	Low-loss dielectric	Rigid	mm-Wave	Moderate
Proposed Antenna (CPW Feed)	22.5× 22.5 × 0.1 mm^2	-24.5dB @5.2 GHz, -13.5dB @9.2GHz, and -23.4 GHz	Liquid Crystal Polymer (LCP) type substrate	Flexible	5G WLAN, WiFi, X-band radar, 5G mm-wave, and Ku/K/Ka-band satellite	Simple

In Table 4, comparative analysis of the proposed CPW-fed flexible antenna against previously reported antenna designs for dimensions, return loss, substrate material, flexibility, and operational frequency bands.

CONCLUSION

This study constructed and assessed a small, flexible antenna for multiband millimeter-wave applications using a liquid crystal polymer (LCP) substrate. The suggested antenna achieves three broad operating bands, covering 4.879–5.513 GHz, 8.394–10.006 GHz, and 13.864–39.892 GHz, with corresponding fractional bandwidths of 12.21%, 17.51%, and 96.8%, respectively, by using a single-port coplanar waveguide (CPW) feed structure. Excellent impedance matching across all bands is confirmed by the simulated findings, proving that LCP is a suitable substrate material for flexible and high-frequency electronic platforms. Bending studies at radii of 10 mm, 30 mm, and 50 mm demonstrated only slight resonance shifts and maintained impedance performance, confirming mechanical robustness. These results demonstrate that the suggested antenna, which combines broad bandwidth, dependable matching, and structural flexibility, is a good contender for conformal and wearable millimeter-wave systems. These findings verify that the suggested LCP-based antenna is a viable option for wearable, conformal, and small high-frequency communication devices.

REFERENCES

1. Li L, Zhang X, Yin X, Zhou L. A compact triple-band printed monopole antenna for WLAN/WiMAX applications. IEEE Antennas Wirel Propag Lett. 2016;15:1853–5.
2. Kumar VV, Kumar MS. Analysis of gain pattern in square patch reconfigurable antenna on FR4 substrate and compared with RT/duroid for wireless application. AIP Conf Proc. 2024;3193(1):020184.
3. Sudheer V, Raja A, Thiruchelvam V, Deepak A. Comparative analysis on bandwidth enhancement of innovative T shape isotropic antenna using RT duroid substrate with FR4 substrate. AIP Conf Proc. 2024;3161(1):020232.
4. Hasan MM, Hossain MS, Rahman MM, Islam MT. Frequency and bandwidth modulation of a wide band-stop metamaterial for EMI shielding applications. Opt Laser Technol. 2024;172:110515.
5. Nasir N, Jamaluddin MH, Hidayu N, Ahmad H, Abbas SM. A dual broadband substrate integrated waveguide dielectric resonator antenna with T-slot for 5G mmWave applications. In: Proc Int Symp Antennas Propag (ISAP); 2024. p. 1–2.
6. Sun L, Zhang Y, Liu H, Chen X, Wang Z, Li Q. High-gain millimeter-wave stretchable array antenna based on electrospun-BaTiO3/PDMS composite membrane substrate. ACS Appl Mater Interfaces. 2025 Jun 4.
7. Zheng W, Liu Y, Chen Z, Huang J, Xu K, Wang H. A broadband metasurface-loaded leaky-wave antenna based on SICL with suppressed open stopband and enhanced efficiency for millimeter-wave applications. IEEE Antennas Wirel Propag Lett. 2025 Aug 5.
8. Ananta RA, Pratama Y, Setiawan D, Nugroho A, Firmansyah T. Regression machine learning-based highly efficient dual band MIMO antenna design for mm-wave 5G application and gain prediction. Sci Rep. 2025;15(1):28730.
9. Farahat AE, Hussein KF. High-gain wide-band Yagi–Uda antenna for millimeter-wave applications. IEEE Access. 2025 Apr 30.
10. Gayathri KP, Shanmuganantham T. Interdigitated comb slot substrate integrated waveguide for millimeter wave communication. In: Proc Int Conf Next Gener Commun Inf Process (INCIP); 2025. p. 650–4.
11. Paul S, Azad AR, Nandi D. Compact microstrip patch antenna loaded with dual slits for 5G millimeter-wave applications. In: Proc IEEE Silchar Subsection Conf (SILCON); 2024. p. 1–4.
12. Tiwari P, Kaushik M, Shastri A, Gahlaut V. Quad-port planar MIMO antenna with wideband capabilities for millimeter-wave 5G Ka-band applications. Phys Scr. 2025;100(4):045016.
13. Liu F, Xu K, Zhao P, Dong L, Wang G. Uniplanar dual-band printed compound loop antenna for WLAN/WiMAX applications. Electron Lett. 2017;53(16):1083–4.
14. Hussain R, Abou-Khousa M, Iqbal N, Algarni A, Alhuwaimel SI, Zerguine A, Sharawi MS. A multiband shared-aperture MIMO antenna for millimeter-wave and sub-6 GHz 5G applications. Sensors. 2022;22(5):1808.

15. Sun L, Li Y, Zhang Z, Feng Z. Wideband 5G MIMO antenna with integrated orthogonal-mode dual-antenna pairs for metal-rimmed smartphones. IEEE Trans Antennas Propag. 2020;68:2494–503.
16. Barani IRR, Wong KL, Zhang YX, Li WY. Low-profile wideband conjoined open-slot antennas fed by grounded coplanar waveguides for 4×4 5G MIMO operation. IEEE Trans Antennas Propag. 2020;68:2646–57.
17. Li S, Chi T, Wang Y, Wang H. A millimeter-wave dual-feed square loop antenna for 5G communications. IEEE Trans Antennas Propag. 2017;65:6317–28.
18. Shirkolaei MM. Wideband linear microstrip array antenna with high efficiency and low side-lobe level. Int J RF Microw Comput Aided Eng. 2020;30:e22412.
19. Alibakhshikenari M, Babaeian F, Virdee BS, Aissa S, Azpilicueta L, See CH, Althuwayb AA, Huynen I, Abd-Alhameed RA, Falcone F. A comprehensive survey on various decoupling mechanisms with focus on metamaterial and metasurface principles applicable to SAR and MIMO antenna systems. IEEE Access. 2020;8:192965–3004.
20. Althuwayb AA. Low-interacted multiple antenna systems based on metasurface-inspired isolation approach for MIMO applications. Arab J Sci Eng. 2021.
21. Ikram M, Nguyen-Trong N, Abbosh A. Hybrid antenna using open-ended slot for integrated 4G/5G mobile application. IEEE Antennas Wirel Propag Lett. 2020;19:710–4.
22. Ikram M, Nguyen-Trong N, Abbosh A. Multiband MIMO microwave and millimeter antenna system employing dual-function tapered slot structure. IEEE Trans Antennas Propag. 2019;67:5705–10.
23. Jilani SF, Munoz MO, Abbasi QH, Alomainy A. Millimeter-wave liquid crystal polymer-based conformal antenna array for 5G applications. IEEE Antennas Wirel Propag Lett. 2018;18(1):84–8.
24. Xiao W, Mei T, Lan Y, Wu Y, Xu R, Xu Y. Triple band-notched UWB monopole antenna on ultra-thin liquid crystal polymer based on ESCSRR. Electron Lett. 2017;53(2):57–8.
25. Garg R, Bhartia P, Bahl I, Ittipiboon A. Microstrip antenna design handbook. Norwood (MA): Artech House; 2001.
26. Hasan MI, Motin MA, Habib MS. Circular ring slotting technique of making compact microstrip rectangular patch antenna for four band applications. In: Proc Int Conf Informat Electron Vis (ICIEV); 2013. p. 1–4.
27. Alipoori S. Advanced polymer composite materials: fabrication techniques, mechanics and diverse applications. Metall Mater Data. 2024;2(3):65–80.
28. Liu H, Wei S, Qiu H, Zhan B, Liu Q, Lu W, Zhang J, Ngai T, Chen T. Naphthalimide-based aggregation-induced emissive polymeric hydrogels for fluorescent pattern switch and biomimetic actuators. Macromol Rapid Commun. 2020;41(13).

